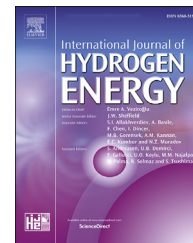




ELSEVIER

Available online at [www.sciencedirect.com](http://www.sciencedirect.com)

ScienceDirect

journal homepage: [www.elsevier.com/locate/he](http://www.elsevier.com/locate/he)

## Combustion features of CH<sub>4</sub>/NH<sub>3</sub>/H<sub>2</sub> ternary blends

S. Mashruk<sup>a</sup>, M.O. Viguera-Zuniga<sup>b</sup>, M.E. Tejeda-del-Cueto<sup>b</sup>, H. Xiao<sup>c</sup>,  
C. Yu<sup>d</sup>, U. Maas<sup>d</sup>, A. Valera-Medina<sup>a,\*</sup>

<sup>a</sup> College of Physical Sciences and Engineering, Cardiff University, UK

<sup>b</sup> School of Engineering, Universidad Veracruzana, Mexico

<sup>c</sup> School of Naval Architecture and Ocean Engineering, Guangzhou Maritime University, China

<sup>d</sup> Institute of Technical Thermodynamics, Karlsruhe Institute of Technology (KIT), Karlsruhe, Germany

### HIGHLIGHTS

- Ternary blends of ammonia/methane/hydrogen are poorly understood.
- Operability maps improve with the content of methane and hydrogen.
- Extinction strain rates suffer considerable relative variation at high ammonia contents.
- High ammonia content blends shift from OH/CH/NH formation to NH<sub>2</sub> at high equivalence ratios.
- There are blends that present low emissions and high operability with low carbon content.

### ARTICLE INFO

#### Article history:

Received 30 January 2022

Received in revised form

21 March 2022

Accepted 25 March 2022

#### Keywords:

Hydrogen

Ammonia

Combustion

Gas turbines

Chemiluminescence

Emissions

### ABSTRACT

The use of so-called “green” hydrogen for decarbonisation of the energy and propulsion sectors has attracted considerable attention over the last couple of decades. Although advancements are achieved, hydrogen still presents some constraints when used directly in power systems such as gas turbines. Therefore, another vector such as ammonia can serve as a chemical to transport and distribute green hydrogen whilst its use in gas turbines can limit combustion reactivity compared to hydrogen for better operability. However, pure ammonia on its own shows slow, complex reaction kinetics which requires its doping by more reactive molecules, thus ensuring greater flame stability. It is expected that in forthcoming years, ammonia will replace natural gas (with ~90% methane in volume) in power and heat production units, thus making the co-firing of ammonia/methane a clear path towards replacement of CH<sub>4</sub> as fossil fuel. Hydrogen can be obtained from the pre-cracking of ammonia, thus denoting a clear path towards decarbonisation by the use of ammonia/hydrogen blends. Therefore, ammonia/methane/hydrogen might be co-fired at some stage in current combustion units, hence requiring a more intrinsic analysis of the stability, emissions and flame features that these ternary blends produce. In return, this will ensure that transition from natural gas to renewable energy generated e-fuels such as so-called “green” hydrogen and ammonia is accomplished with minor detrimental towards equipment and processes. For this reason, this work presents the analysis of combustion properties of ammonia/methane/hydrogen blends at different concentrations. A generic tangential swirl burner was employed at constant power and various equivalence ratios. Emissions, OH\*/NH\*/NH<sub>2</sub>\*/CH\* chemiluminescence, operability maps and spectral signatures were obtained and are discussed. The extinction behaviour has also been investigated for strained laminar premixed flames. Overall, the change from fossils to e-fuels is led by the shift in reactivity of radicals such as OH, CH, CN and NH<sub>2</sub>, with an

\* Corresponding author.

E-mail address: [valeramedinaa1@cardiff.ac.uk](mailto:valeramedinaa1@cardiff.ac.uk) (A. Valera-Medina).

<https://doi.org/10.1016/j.ijhydene.2022.03.254>

0360-3199/© 2022 The Authors. Published by Elsevier Ltd on behalf of Hydrogen Energy Publications LLC. This is an open access article under the CC BY license (<http://creativecommons.org/licenses/by/4.0/>).

increase of emissions under low and high ammonia content. Simultaneously, hydrogen addition improves operability when injected up to 30% (vol), an amount at which the hydrogen starts governing the reactivity of the blends. Extinction strain rates confirm phenomena found in the experiments, with high ammonia blends showing large discrepancies between values at different hydrogen contents. Finally, a 20/55/25% (vol) methane/ammonia/hydrogen blend seems to be the most promising at high equivalence ratios (1.2), with no apparent flashback, low emissions and moderate formation of  $\text{NH}_2/\text{OH}$  radicals for good operability.

© 2022 The Authors. Published by Elsevier Ltd on behalf of Hydrogen Energy Publications LLC. This is an open access article under the CC BY license (<http://creativecommons.org/licenses/by/4.0/>).

## Introduction

One of the most critical problems humanity faces is climate change, a global problem triggered by the increase in  $\text{CO}_2$  emissions towards the atmosphere product of fossil fuels combustion. Therefore, governments, researchers and technologists have concentrated their efforts in finding solutions to the production of these emissions whilst keeping current systems operational. One method to achieve this objective is by replacing fossil fuels with other so-called “greener” substitutes. “Electro-fuels” (e-fuels), products of electrolysis generated via renewable energies (i.e. solar, wind and marine), seem to be a real, short-term solution [1]. Out of all the options, so-called “green” hydrogen, a well-studied e-fuel, has the potential to be burned without generating large amounts of emissions harmful for the environment. However, several challenges remain with the use of pure hydrogen for distribution of renewable energy. According to the Hydrogen Council [2] the distribution of hydrogen can be accomplished using other vectors such as Liquid Organic Hydrogen Carriers (LOHC), ammonia ( $\text{NH}_3$ ) or even Liquefied hydrogen (LH). In a comparison for long distance distribution, the cost of using LOHC,  $\text{NH}_3$  and LH was 3.5–4.4, 3.5–4.4 and 3.2–3.8 US\$/ $\text{kg}_{\text{H}_2}$  transported, respectively. However, the ammonia case includes a cost of 0.9–1.6 US\$/ $\text{kg}_{\text{H}_2}$  transported allocated to cracking the molecule to recover hydrogen. Thus, the avoidance of cracking with the direct use of ammonia for power applications could reduce the cost of transporting hydrogen to values  $\sim 2.0$  US\$/ $\text{kg}_{\text{H}_2}$  transported over long distances.

In terms of the power sector, the use of pure ammonia instead of hydrogen (which can be obtained from cracked ammonia) presents several advantages apart from just the reduction in costs. It is estimated that  $\sim 8$ –10% of the efficiency of large power systems such as gas turbine-based combined cycles would be needed for the cracking process to reach hydrogen purities  $>99\%$  [3]. Having an estimated efficiency  $\sim 60\%$  using pure ammonia, these cycles could potentially compete with current fossil cycles, whilst the use of fully cracked hydrogen will impact not only distribution costs but also final efficiencies. Further, the reactivity and diffusivity of pure hydrogen combustion in these equipment is still a technological challenge [4]. Therefore, ammonia on its own presents an interesting option to replace fossils in gas turbine systems.

However, the use of pure ammonia presents its own obstacles. It is well-known that pure ammonia combustion leads to low laminar burning velocities [5], hence requiring larger systems or improved methods to enhance residence times and energy exchange. Laminar burning velocities in the range of 2–8 cm/s have been documented in a large number of studies [6], which are an order of magnitude lower than those expected from methane-based flames. Although the increase in inlet temperature can increase this value, the increase in pressure levels down this uplifting effect, bringing back to single digits ( $<8$  cm/s) the laminar burning velocity of pure ammonia blends [7]. As a consequence, the effect can lead to conditions where blowoff is difficult to control [8]. Similarly, the ignition energy of ammonia is several orders of magnitude higher than for hydrogen (8.000 mJ compared to 0.011 mJ [9,10]), whilst high ammonia blends have also high ignition delay times [11], impacting directly the combustion process. Therefore, although several programs are currently evaluating the use of pure ammonia for low power conditions using concepts such as MILD combustion [12] and direct liquid injection [13], to large industrial power units in the range of MWs [14], it is probable that the concept will require major retrofitting, additional post-combustion emissions treatment or a change in combustion philosophy, thus demanding an additional step towards the transition to pure ammonia.

One concept that could preclude the use of pure ammonia and that is currently under large scrutiny is the use of doping agents such as methane or hydrogen to boost the reactivity of ammonia blends, increasing laminar burning velocities to achieve better combustion stability without major changes to the combustion chambers. In the case of methane, the chemical is the main component of natural gas that is used in most gas turbines worldwide. Reports from various sources [1,15–17] denote the increase of laminar burning velocities in ammonia/methane blends to values close to those of pure methane, whilst analyses show regions of relatively low  $\text{CO}$ /low unburned ammonia emissions close to 1.05 equivalence ratios [18–21]. Furthermore, hydrogen doping has gained considerable attention due to its decarbonising potential. Ammonia/hydrogen blends have also been studied at various concentrations by several groups, where the laminar burning velocity is considerably increased with hydrogen addition, reaching values close to methane with a moderate addition of hydrogen [6,22–24]. Flame stability has also shown

considerable improvement, especially when values between 20 and 40% (vol) hydrogen addition are employed [25–27], as higher concentrations tend to shift the reaction towards hydrogen, generating two reaction zones [26] that also impact on instabilities such as boundary layer flashback [28], reducing operability. Some studies have also shown the shift of the laminar burning velocity towards richer equivalence ratios [11], a phenomenon that can be advantageous for various injection strategies. The use of these blends has also been examined in complex power cycles, demonstrating good numerical performance via multi-stage combustion [29] or post-combustion in external furnaces [30], delivering efficiencies close to 60% as predicted by Cesaro et al. [3,31]. Experimental analyses of the limits of ammonia flames doped with hydrogen and/or methane have been expanded over the years, with details that include not only operability limits [32] but also emissions formation [33], injection strategies affecting flame behaviour [34,35], effects of complex combustion systems [36], amongst others.

Further tests also confirm the increase in NO emissions, one of the detrimental effects of using ammonia as a fuel. Khateeb et al. experimentally showed the considerable formation of NO especially at equivalence ratios  $\sim 0.8$  when using various methane or hydrogen doping contents [25,37]. Similar trends have also been found by others [20,38,39], denoting that the pools of OH/O/H radicals critically impacts the formation of NO via HNO mainly. Recent studies also suggest the impact of flame curvature in the formation of NO as preferential diffusion of H<sub>2</sub> into convex-shaped portions of the flame occur [40]. If methane blends are employed, CO and/or CO<sub>2</sub> can also be formed via competition between OH, HCO and C<sub>*n*</sub>H<sub>*x*</sub> species [41,42]. Further attempts have also used very lean combustion conditions for the use of ammonia blends. Khateeb et al. [25,43] demonstrated that the production of NO emissions below 0.6 equivalence ratio was below one single digit, whilst OH formation was considerably decreased under these conditions, thus reducing fuel NO productions. However, another important emission, nitrous oxide (N<sub>2</sub>O), was revealed in those tests, accounting for a considerable percentage in the exhaust emissions of such a combustion chamber [25]. Similarly, other works have revealed the formation of this pollutant (ie. with  $\sim 300$  times the Greenhouse Warming Potential of CO<sub>2</sub>) at very lean conditions, questioning the applicability of such a concept [44,45]. Simultaneously, the work on rich conditions has demonstrated that NO and N<sub>2</sub>O decrease considerably as equivalence ratios between 1.10 and 1.25 are employed, a phenomenon that links the production of NH<sub>2</sub> and NH radicals at lower temperatures, then leading to reaction paths through NNH, H<sub>2</sub>O and N<sub>2</sub> formation that supersede the NO formation path, especially in post-combustion zones [46,47]. However, it is clear that further research is needed to untangle the production of species such as N<sub>2</sub>O in ammonia flames [48–50].

Therefore, increasing amount of work exists on the use of these two doping agents. However, and as part of the transition to the use of ammonia in gas turbines and engines, it is likely that practical applications will start on methane gas, transitioning to ammonia and hydrogen, hence reducing retrofitting whilst maximising the lifespan of currently operating units. This is evident in some of the latest

demonstration systems designed to use methane but that have been retrofitted for ammonia/hydrogen blends [51–54]. Therefore, with a vast number of units that can be potentially retrofitted to use ammonia, it is likely that the three chemicals might be at some point co-fired simultaneously in these systems.

Therefore, this work presents the analysis of ternary NH<sub>3</sub>/CH<sub>4</sub>/H<sub>2</sub> blends under atmospheric conditions and constant power. The work starts with the definition of operability maps similar to those produced for binary blends [25,37,55]. An industrial representative tangential swirl burner was employed. The work then focuses on specific blends. A numerical analysis that evaluates the impacts of these blends on extinction strain rate (ESR) for the strained premixed laminar flame is performed, followed by experiments that obtained chemiluminescence features of major radicals (OH\*, CH\*, NH\* and NH<sub>2</sub>\*). Results are compared between cases, whilst spectral results and emission analyses are also shown for NO<sub>x</sub> and unburned ammonia in the flue gases. It is intended that these results guide potential ammonia users towards the transition of ammonia/hydrogen blends whilst using their current natural gas systems.

## Methodology

### Experimental set-up

The experiments employed a tangential swirl burner, with a geometrical swirl of 1.08, at atmospheric pressure and inlet temperature of 288 K, Fig. 1. The burner was supplied with fully premixed mixtures of ammonia, methane and hydrogen. Ammonia was varied from 0 to 100%, whilst hydrogen was only varied from 0 to 30% (vol) and methane was the rest. Flashback was defined when the flame fully retreated inside of the premixing chamber, whilst blowoff (lean and rich) was defined when the flame was fully detached and lost from the burner mouth. Bronkhorst mass flow controllers, EL-FLOW select with a precision of 0.5% within a range of 15–95% mass flow were used for the three chemicals. Air was also provided without preheating via a Bronkhorst mass flow controller. Various equivalence ratios were selected for the definition of operability maps. An 8 kW constant power was kept for comparisons.

Selected points, Table 1, were further investigated using numerical modelling of extinction strain rates, chemiluminescence, emissions analyses and spectral signatures. A constant equivalence ratio of 1.20 was selected on the basis of previous experimental campaigns and modelling results that demonstrated the high potential of this condition for both emissions abatement and flame control [56].

Nitric oxides (NO, NO<sub>2</sub>, N<sub>2</sub>O), water content, oxygen percentage and ammonia concentration were measured using a bespoke Emerson CT5100 Quantum Cascade Laser analyser at a frequency of 1 Hz, a repeatability of  $\pm 1\%$ , 0.999 linearity, and a sampling temperature of 190 °C. A heated line set at 160 °C was employed to avoid condensation of water vapor. Emissions are presented with a 15% oxygen correction. A simple Logitech C270 webcam was used to monitor the flame stability at a distance of 5 m.

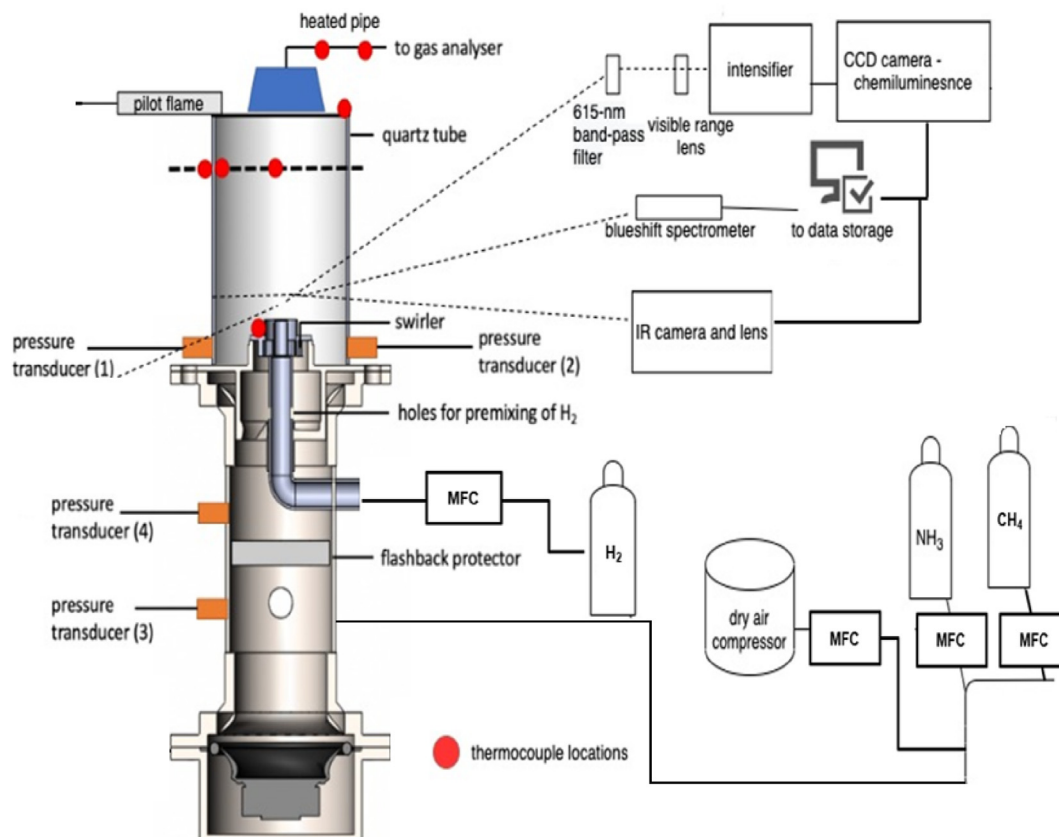


Fig. 1 – Tangential combustor with measuring techniques and control systems.

A pair of LaVision CCD cameras were employed to obtain chemiluminescence traces of various species. The units were triggered simultaneously at a frequency of 10 Hz and a gain of 85%. Various Edmond filters were used for each species of interest, namely OH\* (309 nm) [57], NH\* (336 nm) [57–60], CH\* (430 nm) and NH<sub>2</sub>\* (630 nm) [57,61]. LaVision Davis v10 was used to gather 500 frames per flame, which were then post-processed using a bespoke MatLab script [62] designed to conduct Abel Deconvolution after 3 × 3 pixel median filter and temporary averaging 500 images. Finally, a Blue-Wave StellarNet CMOS spectrometer with a detector ranging from 200 to 1100 nm was focused on the flame core to measure the emission spectrum during the combustion process.

### Numerical set-up

The extinction strain rate for the laminar flame in counterflow configurations is an important quantity to describe under which the flow can still get a stable burning flame. Therefore, the numerical simulation for the prediction of extinction strain rates (ESR) for strained premixed laminar flames can provide an insight into the effect of blending in the proposed ternary blends. For that effect, ESRs are obtained by using the INSFLA code [63]. The code solves the governing equation for mass, species and energy based on the two-parameter formulation proposed in Ref. [64], and a detailed transport model including thermal diffusion (Soret effect) is considered. The code has been successfully applied for the prediction of ESRs for non-premixed counterflow flames [65]. The chemical

kinetics used is the detailed chemical kinetics from Li et al. [66], which includes 128 species and 957 reaction steps. In that work, the chemical kinetics has been tested for a wide range of application (ignition delay times, laminar burning velocity, 2-D non-premixed turbulent flame) with different levels of H<sub>2</sub> and CH<sub>4</sub> additions. Atmospheric pressure and inlet temperature (300 K) and a constant equivalence ratio of 1.2, were considered consistent with the experiments.

## Results and discussions

### Stability limits

Initial operability maps using binary flames, Figs. 2 and 3, show how the increase in ammonia concentration reduces operability. As anticipated and seen in other works, the use of hydrogen provides a larger operability limit than methane. The high reactivity and diffusivity of the hydrogen molecule is culprit for this behaviour. Interestingly, the ammonia/hydrogen blend suffers an unexpected shift in combustion dynamics passed the 70% (vol) ammonia content. High hydrogen content (>30%) leads to flashback (FB), whilst higher ammonia blends (<30% hydrogen content) produce lean blowoff (LBO) conditions at low equivalence ratios. The result, in accord with other works that have found that a 70-30% (vol) ammonia-hydrogen blend is considerably more stable than other conditions [67], confirms also the numerical findings from Valera-Medina et al. [26] that denote the formation of

**Table 1 – Measured points. Methane concentration was reduced whilst increasing ammonia and hydrogen.**

| TP | CH <sub>4</sub> /NH <sub>3</sub> /H <sub>2</sub> (vol%) | CH <sub>4</sub>        |                        | NH <sub>3</sub>        |                        | H <sub>2</sub>         |                        | Air                    |                        | Equivalence ratio ( $\phi$ ) | Power (kW) |
|----|---|------------------------|------------------------|------------------------|------------------------|------------------------|------------------------|------------------------|------------------------|------------------------------|------------|
|    |   | Vol. flow rate (L/min) | Vol. flow rate (L/min) | Vol. flow rate (L/min) | Vol. flow rate (L/min) | Vol. flow rate (L/min) | Vol. flow rate (L/min) | Vol. flow rate (L/min) | Vol. flow rate (L/min) |                              |            |
| 1  | 70/30/10  | 12.25                  | 3.5                    | 1.75                   | 111.5                  | 1.2                    | 8                      |                        |                        |                              |            |
| 2  | 60/30/10  | 11.4                   | 5.7                    | 1.9                    | 111.6                  | 1.2                    | 8                      |                        |                        |                              |            |
| 3  | 50/35/15  | 10.37                  | 7.26                   | 3.11                   | 110.5                  | 1.2                    | 8                      |                        |                        |                              |            |
| 4  | 40/40/20  | 9.16                   | 9.16                   | 4.58                   | 109.5                  | 1.2                    | 8                      |                        |                        |                              |            |
| 5  | 30/50/20  | 7.64                   | 12.73                  | 5.09                   | 109                    | 1.2                    | 8                      |                        |                        |                              |            |
| 6  | 20/55/25  | 5.76                   | 15.84                  | 7.2                    | 107.6                  | 1.2                    | 8                      |                        |                        |                              |            |
| 7  | 10/65/25  | 3.28                   | 21.35                  | 8.21                   | 106.3                  | 1.2                    | 8                      |                        |                        |                              |            |
| 8  | 0/70/30   | 0                      | 27.05                  | 11.59                  | 103.9                  | 1.2                    | 8                      |                        |                        |                              |            |
| 9  | 0/75/25   | 0                      | 28.6                   | 9.53                   | 104.4                  | 1.2                    | 8                      |                        |                        |                              |            |

two flame fronts, one driven by hydrogen at the root of the flame, followed by a second, longer inner flame trapped within the shearing flow and the central recirculation zone of such a combustor. This in turn, leads to the onset of FB and lower stability under lean conditions.

When ternary blends were employed, the operability features changed considerably. For the case with low hydrogen content, Fig. 4, a 10% (vol) hydrogen addition ensures very consistent operability trends. The only observed instabilities are those generated by blowoff, with a system that never experienced FB. Behaviour from  $\Phi = 0.5$  to 1.7 remained relatively linear with small variations in blowoff values, whilst a high reactivity blend such as 80/10/10% (vol) CH<sub>4</sub>/NH<sub>3</sub>/H<sub>2</sub> appears to have slightly higher operability limits than a 0/90/10% (vol) CH<sub>4</sub>/NH<sub>3</sub>/H<sub>2</sub> flame, a phenomenon still not fully understood. However, compared to the binary methane/ammonia blend, the operability of this case has considerably improved especially at high ammonia concentrations, see Fig. 2.

The increase in hydrogen content to 20% (vol) led to the onset of flashback profiles at very low ammonia concentrations, an expected behaviour. However, once passed the 10% (vol) ammonia content, the operability range of the blend performed better than at 10% (vol) hydrogen, compare Figs. 4 and 5. The blend denotes wider LBO limits, with more consistent and also greater Rich Blowoff (RBO) conditions. Further, similar to the previous case, the high ammonia content case (80% vol) showed higher resistance to RBO. The phenomenon could be a consequence of a competition between species [26,28], changes in heat release rates and impacts on coherent structures known to stabilize the flame [8], a phenomenon that requires further investigation. As denoted with the binary flames, there is a point in which one of the fuels overtakes the other, hence shifting the overall chemistry of the combustion profile. This phenomenon should be also occurring with ternary blends. However, the effects over operability seem to be balanced across the different equivalence ratios and ammonia percentages.

Finally, the case with 30% (vol) hydrogen was also analysed, Fig. 6. As expected, the case provided the widest operability range. However, different to the previous cases, the change in ammonia and hydrogen content produced marked differences between operability points. Initially, flashback occurs at low ammonia content (<40% vol). The low power outputs, hence lower Re, would give way to the retreat of the flame via boundary layer flashback, phenomenon with similitude to non-swirling conditions and that is currently under scrutiny elsewhere [28]. However, as this point was passed and ammonia contents in the fuel blends increased beyond 40%<sub>VOL</sub>. (thus methane contents was reduced below 30%<sub>VOL</sub>), the overall flame speed of the blends decreases, leading to the avoidance of flashback. Further, the operability almost doubled when methane was removed from the blend (i.e., 0/70/30 vol.% CH<sub>4</sub>/NH<sub>3</sub>/H<sub>2</sub>) although flashback was observed again. From the stability maps for ammonia/hydrogen blends in Fig. 3, LBO was observed for  $X_{\text{NH}_3} > 0.7$ . To investigate this phenomenon further, this particular blend was repeated numerous times over different days. FB was observed most of the times, while LBO was observed occasionally. Previous research [26] has shown a layer of H<sub>2</sub> flame visible in NH<sub>3</sub>/H<sub>2</sub> blends. Two flames are clearly depicted in these cases. It is

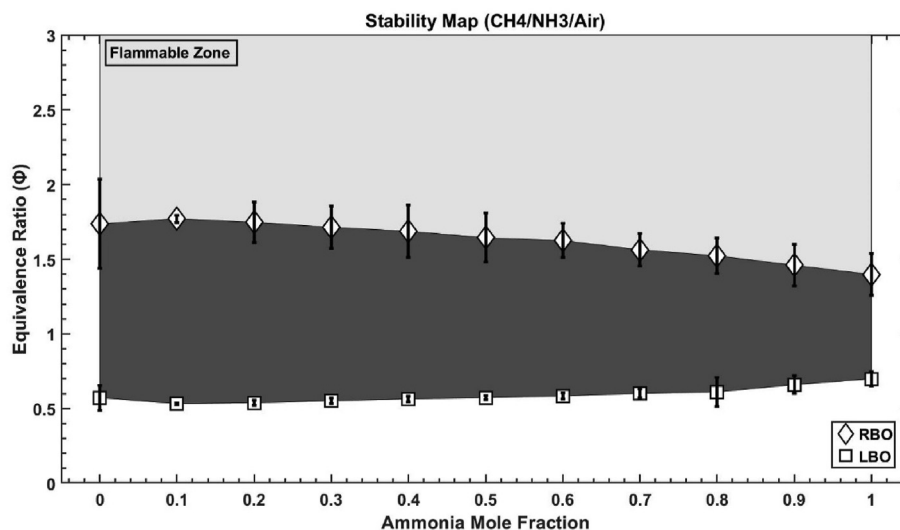


Fig. 2 – Stability map of methane/ammonia flames.

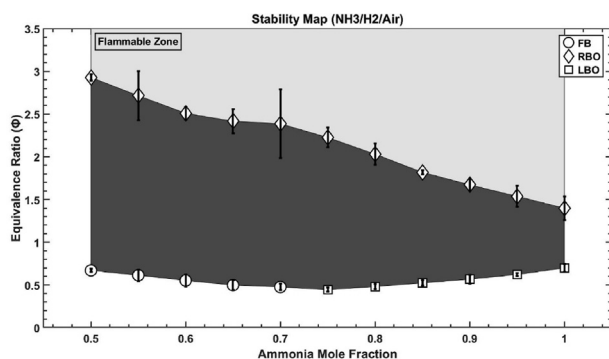


Fig. 3 – Stability map of ammonia/hydrogen flames.

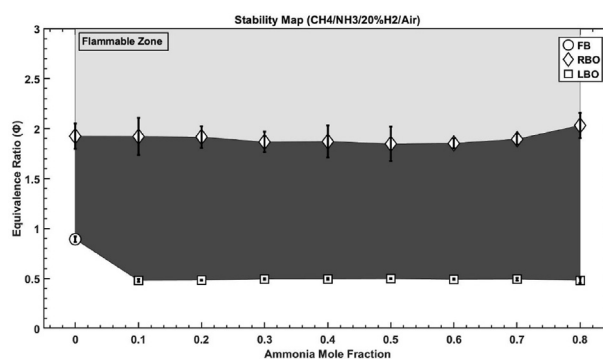


Fig. 5 – Stability map of methane/ammonia/20% (vol) hydrogen flames.

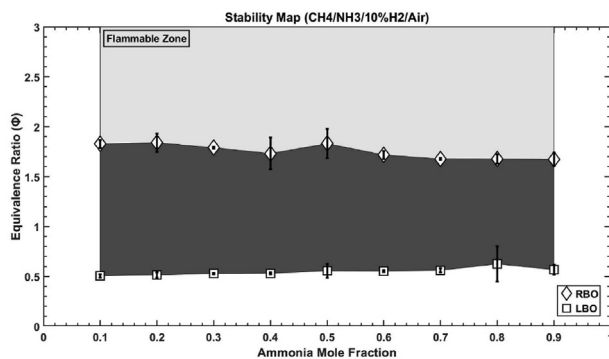


Fig. 4 – Stability map of methane/ammonia/10% (vol) hydrogen flames.

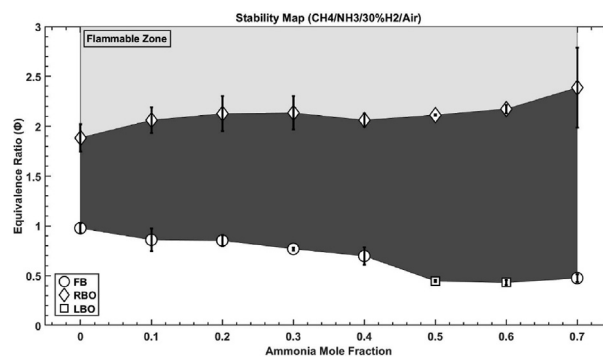


Fig. 6 – Stability map of methane/ammonia/30% (vol) hydrogen flames.

believed this is the reason for the fluctuating instabilities between FB and LBO at the 70/30 vol.%  $\text{NH}_3/\text{H}_2$  point, as the flame under this condition has no  $\text{CH}_4$  content. Hydrogen became the sole fuel with high flame speed. Simultaneously, it has been noticed through this work with ternary blends that the presence of  $\text{CH}_4$  at low percentages in the blends can restrict overall flame reactivity, thus showing LBO. This appears to be a consequence of a competing interaction between molecules

for available oxygen, which combined with the complex nitrogen reactivity from ammonia might be triggering combustion features that need to be further understood. Without the presence of  $\text{CH}_4$  in the blend,  $\text{H}_2$  controls the flame reactivity to a greater extent and thus displayed FB most times for the 70/30 vol.%  $\text{NH}_3/\text{H}_2$  blend. Thus, it is emphasized that this point and those at 0.5 and 0.6 ammonia fraction, Fig. 6, which were

consistently showing LBO, need further study to fully determine their unstable nature and the phenomena triggering this competing relationship.

### Extinction strain rate analyses (numerical)

The flame can become unstable, if the flow is governed by intense turbulence. Commonly, flows with higher turbulence intensity impose higher strain rates to the flame, which may lead to local flame extinction [68]. Furthermore, the change of the flame strain rate also affects the flame propagation velocity. As studied in Ref. [69], in particular, spherical flame fronts cannot propagate if the strain rate increases with increasing flame radius during flame propagation. Therefore, understanding of the effect of the extinction limit on the flame properties will elaborate the interpretation of the flame instability, and compare the flame stability in respect to flame extinction. In other word, extinction strain rates are a good measure for the sensitivity of flame extinction with respect to mixture composition.

Therefore, selected cases, denoted in Table 1, were studied further. Extinction strain rate (ESR) analyses, Fig. 7, show how the flame has a stronger resistance to extinction with increasing addition of H<sub>2</sub> and CH<sub>4</sub>, an expected behaviour which is a consequence of the higher reactivity and larger flame velocity of these two molecules. However, low methane content cases show greater relative deviation ( $(ESR_{X\%H_2} - ESR_{0\%H_2})/ESR_{0\%H_2}$ ) between ESRs obtained at 0% hydrogen and those with some hydrogen content (10, 20 or 30% vol), whilst higher methane content cases denote lower deviations between scenario, Fig. 8. As methane content reaches ~40% (vol), deviations between cases with and without hydrogen remain almost constant, a trend that can be linked to the shift in reactivity. As in previous lines, the reactivity of these ternary blends shift to a different molecule based on the content of the latter, phenomenon that can be traced also to ESR effects. As hydrogen is increased in high ammonia content blends, ESR considerably increases. However, as ammonia is decreased and methane takes over the reaction, further addition of methane does not produce a relatively acute change with the base case (ie. 0% (vol) H<sub>2</sub>) under those conditions. Further, the addition of 10 or 20% (vol) hydrogen has a minor effect than the 30% (vol) cases, which produces an ESR jump greater than 3.5 times from the base case. The effect might be in accord to recent findings by Zitouni et al. [70], who

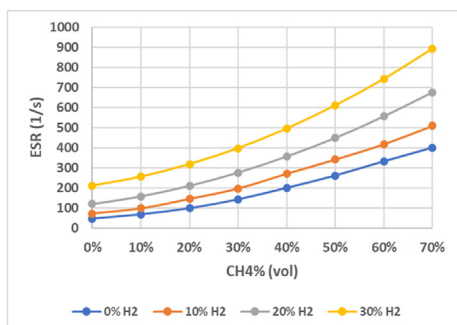


Fig. 7 – ESRs using various blends at 1.20 equivalence ratio.

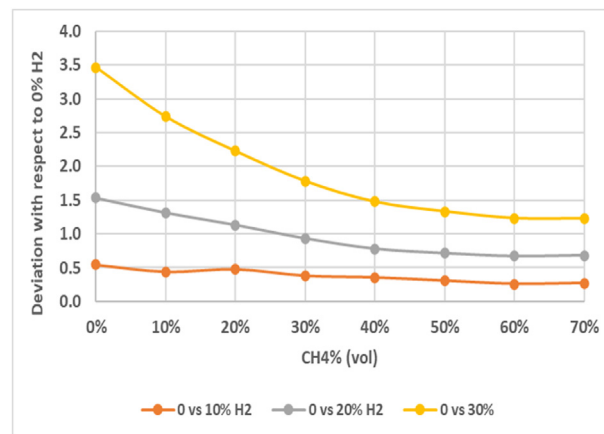


Fig. 8 – ESRs relative deviation from base line at 0% H<sub>2</sub>.

found that the addition of up to 20% hydrogen in ammonia blends is still comparable to 20% methane in terms of laminar burning velocity. However, passing that point and >30% H<sub>2</sub>, the reactivity of binary blends changes abruptly. Further analyses are required to entangle these effects on ternary blends with less than 40% methane.

### Chemiluminescence, spectral signals and emissions (experimental)

Employing intrinsic chemiluminescence analyses, spectral signatures and emissions analyses at constant equivalence ratio (1.2), experimental results were also gathered. Chemiluminescence analyses were normalised to the highest intensity of respective datasets to demonstrate the distributions of radicals in flames and changes in flame topology. Spectral signatures were obtained for these special cases at the range of 200–700 nm.

Chemiluminescence results, Fig. 9, show how the change in fuel content shifts the production of OH\*, CH\*, NH\* and NH<sub>2</sub>\*. Radical production shift towards the top of the flames as ammonia percentages increases due to the increasing flame thickness. OH\*, CH\* and NH\* production decreases with increasing ammonia contents in the fuel while NH<sub>2</sub>\* formation increases, a point detailed in Fig. 10 through spectral analyses.

If the ammonia content remained low, the production of OH\* was enhanced. In parallel, the high signal from CH\* is a consequence of the high methane content (Fig. 9, TP1). Interestingly, NH\* shows the strongest signal amongst cases at this point. It is well-known that NH forms mainly from the reaction  $NH_2 + OH \rightarrow NH + H_2O$  [71], whilst the CH\* marker is employed to determine heat release rates [72]. Having the highest OH\*, CH\* and NH\* signals, the production of NH<sub>2</sub> is overtaken by its reaction to form NH at higher heat release rates (product of OH and CH production). Furthermore, H<sub>2</sub>O and other oxygen containing species could be dissociating, hence increasing the OH\* presence.

As the ammonia content is increased and methane is reduced, a similar reduction trend follows for the three previous radicals with less intensity at the core of the flame. Meanwhile, NH<sub>2</sub>\* increases its signal up to a point that the

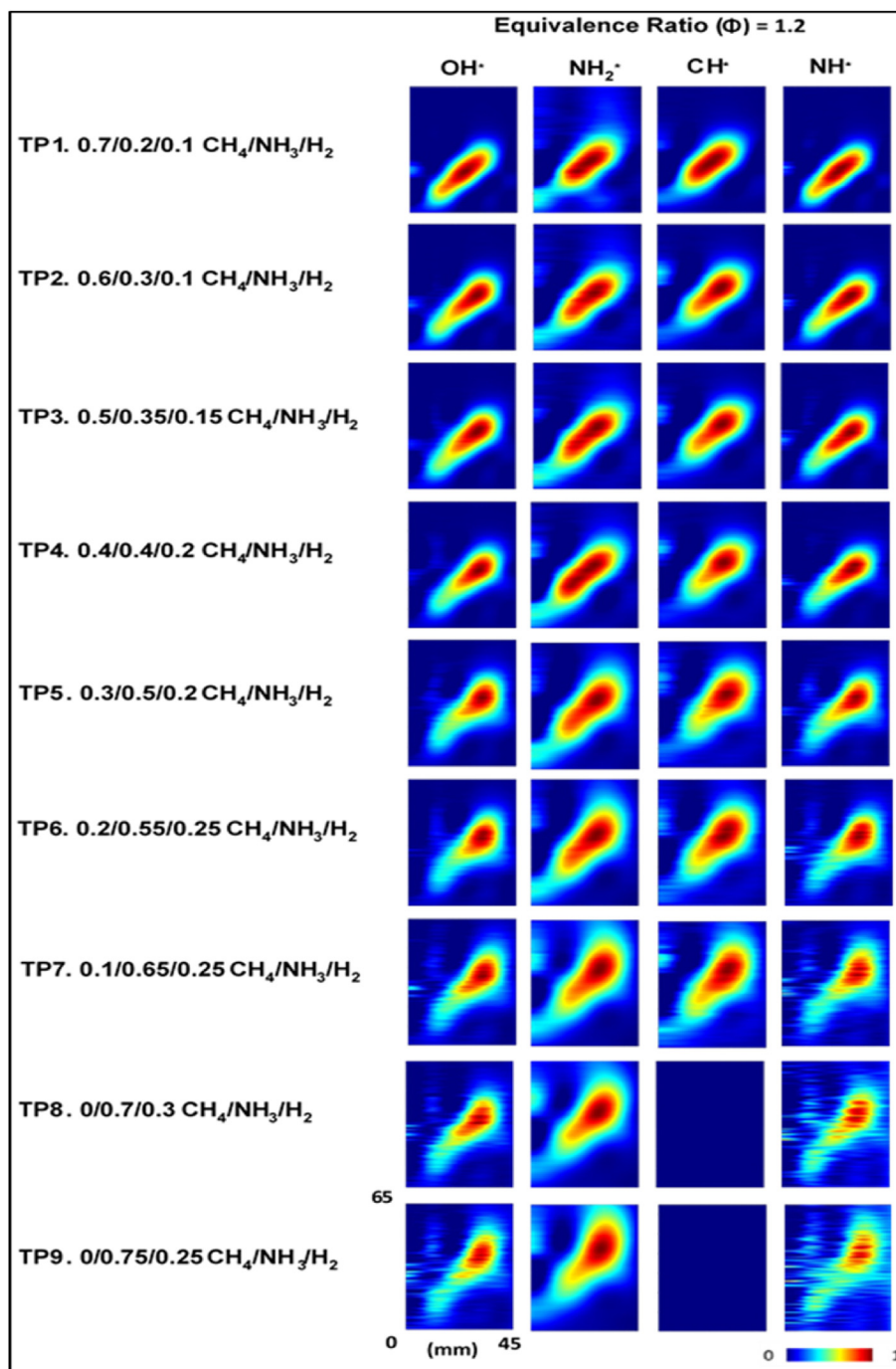


**Fig. 9** – OH\*/NH<sub>2</sub>\*/CH\*/NH\* Chemiluminescence of methane/ammonia/hydrogen flames. Colourmap normalised to image dataset maximum.

latter overtakes any other signal in the field. It is also apparent that the rich conditions have led to a depletion of oxygen, hence OH, that is potentially consumed at the flame front to produce NH<sub>2</sub> from NH<sub>3</sub> + OH reactions. Different to the case with high methane content, Fig. 9 (TP1), where the flame is close to the burner exit, the NH<sub>2</sub>\* signal is now further downstream showing a slower reaction rate with a more distributed flame. Therefore, the competing effect between species, the higher dissociation and the shorter flames in high methane flames appear as a limiting factor in the overall

stability with these blends that does not occur in binary blends. These trends are observed in both the spectral analyses and chemiluminescence results. The productions of OH\*, NH\* and CH\* decrease with decreasing methane content in the fuel due to reducing unavailability of carbon atoms. Low ammonia content cases increase the production of these radicals, whilst the visibility of NH<sub>2</sub> radicals is suppressed. As ammonia is increased, NH<sub>2</sub> intensity also augments, overshadowing the intensities of other species in the flame front at the highest ammonia contents.



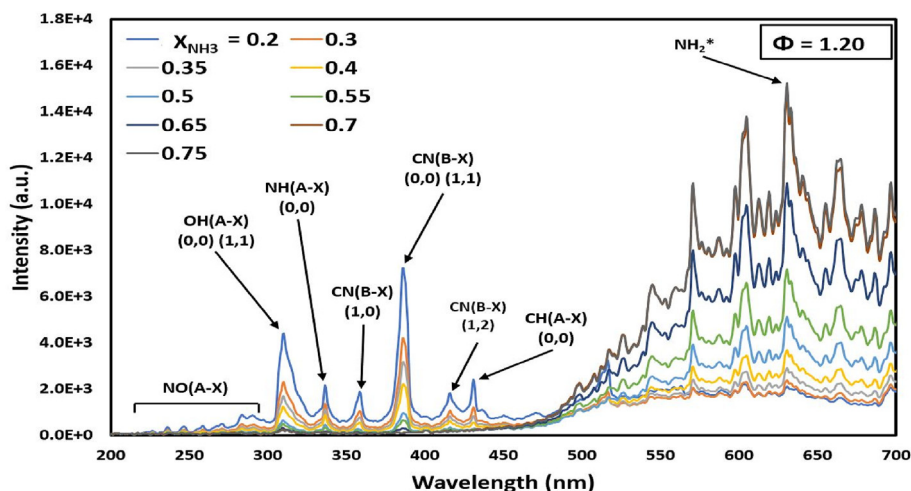


Fig. 10 – Spectral analyses for ternary blends, Table 1.

The low ammonia cases also show higher NO (220–300 nm) production, a point addressed in the emissions analyses. An interesting feature is that CN radicals present monotonic trends to methane content. The presence of CN radicals and NO emissions can lead to the formation of NCO via HCN when oxygen is present [73]. However, this scenario would also lead to high  $N_2O$  emissions which is not present in these cases. Therefore, cyanide-nitrogen, NCN, could be the precursor in the formation of the excessive NO observed with high methane blends [74]. Large pools of reactive N, likely present under these conditions, could be interacting with CN thus forming NO at these equivalence ratios. This mechanism is an important contributor of NO production in hydrocarbon/air flames. Therefore, high methane content scenarios could be leading to the production of thermal, fuel and prompt emissions. This conclusion needs to be studied further using validated reaction mechanisms capable to evaluate the use of ternary blends.

Exhaust emissions for these cases were also obtained, shown in Fig. 11. All cases show a relatively constant  $N_2O$

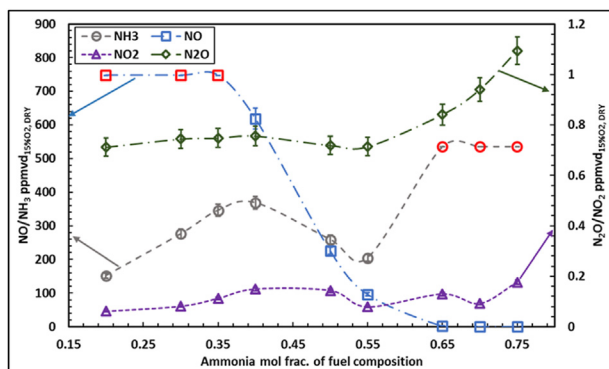


Fig. 11 –  $NO_2$ ,  $N_2O$ ,  $NH_3$  and NO emissions at various ammonia mole fractions. Red symbols are out of range of the QCL analyser. (For interpretation of the references to color in this figure legend, the reader is referred to the Web version of this article.)

trend, with low, limited  $NO_2$  emissions which are also consistent between points. This trend is recurrent at equivalence ratios close to 1.20 [45]. However, unburned ammonia emissions and NO suffer considerable changes depending on the used blends. As expected, high ammonia content cases lead to high unburned ammonia concentrations [75–77], which in some cases are above the maximum measurement ranges of the equipment. Interestingly, ammonia emissions dropped for 30/50/20<sub>VOL.%</sub> and 20/55/25<sub>VOL.%</sub>  $CH_4/NH_3/H_2$  fuel blends. This can be attributed to the balance between decreasing  $CH_4$  and increasing  $H_2$  contents in the fuel blends, which is affecting the productions of H, O and OH radicals which are responsible for ammonia oxidation [29]. Although various studies have shown that 70/30% (vol)  $NH_3/H_2$  blends denote higher efficiency with low emissions, the relatively low power of these experiments, hence high heat losses, lead to lower ammonia consumption at the flame front and in post-combustion regions. However, there are cases where a relatively high methane concentration, i.e., 20/55/25 (vol%)  $CH_4/NH_3/H_2$ , show relatively low unburned ammonia, potentially as a consequence of the greater reactivity of such blends. Simultaneously, the high ammonia concentration in the fuel ensures that NO emissions are reduced under those heat conditions, potentially through reactions such as  $NO + NH_2 \rightarrow N_2 + H_2O$  and those that ensure the path  $NH_2 \rightarrow NH \rightarrow NNH \rightarrow N_2$ .

Simultaneously, the low ammonia content blends denote the highest NO emissions (out of range), Fig. 11. This is a consequence of the higher reactivity due to high methane content and thus greater temperatures which contribute to thermal and prompt (via HCN) NO formation, combined with the inability of the reactions to reduce NO. Additionally, fuel NO is formed through  $NH_2 \rightarrow NH \rightarrow HNO \rightarrow NO$  and other competing reactions such as  $HNO + CO = NH + CO_2$  could be leading to higher NO profiles. High NH concentrations, as observed in the chemiluminescence trends, Fig. 9 (TP1), can lead to both high CO and NO via HNO, thus making these blends unpractical. Therefore, it is clear that the highest performing ternary case in terms of emissions at low power is 20/55/25% (vol%)  $CH_4/NH_3/H_2$  blend that with high ammonia

content and a delicate balance of methane and hydrogen concentrations led to relatively better reactivity which consumes most ammonia whilst boosting the post-reaction of NO emissions. Stability wise, this blend is also relatively stable without flashback propensity.

## Conclusions

An industrial scale tangential swirl burner was employed to investigate stability limits of binary ( $\text{CH}_4/\text{NH}_3$  and  $\text{NH}_3/\text{H}_2$ ) and ternary ( $\text{CH}_4/\text{NH}_3/\text{H}_2$ ) blends at atmospheric conditions. Extinction strain rate analyses were carried out numerically for various ternary blends at  $\Phi = 1.2$  to understand the resistance to extinction with increasing methane and hydrogen contents in the blends. Finally, selected ternary blends at  $\Phi = 1.2$  were analysed in terms of spatially resolved chemiluminescence measurements, exhaust emissions and spectral footprints. The main conclusions of this investigations are summarised as follows.

1. Binary fuels showed reduced stability regions with increasing ammonia contents in the fuel. However, addition of  $\text{H}_2$  with  $\text{NH}_3$  enhances the stability regions considerably more than  $\text{CH}_4$  addition. More than 30% (vol)  $\text{H}_2$  addition introduces flashback in the flames in lean regions due to the introduction of instabilities related to reactivity, heat release rate and change in coherent structures.
2. Three operability maps of ternary blends were reported with 10, 20 and 30% (vol)  $\text{H}_2$ . With the presence of 10% (vol)  $\text{H}_2$ , the operability regions are found to be quite consistent, bounded by blowoff limits. 20% (vol)  $\text{H}_2$  blends displayed better stability regions when the ammonia fraction was above 0.1. Flashback was only observed for methane/hydrogen blend scenario. The 30% (vol)  $\text{H}_2$  blends displayed narrower operability regions up to 40% (vol)  $\text{NH}_3$  due to flashback. Stability region widens considerably past this point as flashback was avoided. Further analyses, at various powers and configurations, are still needed to find general trends applicable to similar tangential swirl burners.
3. Low methane contents in the blends led to greater relative deviations between ESRs while constant deviations were observed with or without  $\text{H}_2$  as methane fraction was  $X_{\text{CH}_4} \approx 0.4$ . ESR considerably increased with increasing  $\text{H}_2$  contents in high ammonia blends. However, this was not the case with reduced ammonia and increased methane contents in the blends. When  $X_{\text{H}_2} = 0.3$ , considerable increase in ESR was observed.
4.  $\text{OH}^*$ ,  $\text{CH}^*$  and  $\text{NH}^*$  formation was found to be decreasing with increasing ammonia contents in the selected ternary blends at  $\Phi = 1.2$ , with increased  $\text{NH}_2^*$  intensity. Lifting of the flame from the burner exit was reported with decreasing methane contents due to slower reaction rate and therefore enhanced distributions of radicals. High NO emissions at exhaust were measured for high methane blends due to higher temperatures and a combination of thermal, prompt and fuel NO formations. Presence of high methane contents in the blends enhanced ammonia oxidation by producing H, O

and OH radicals.  $\text{NO}_2$  and  $\text{N}_2\text{O}$  emissions were found to be negligible across the blends at this rich condition. Finally, 20/55/25% (vol)  $\text{CH}_4/\text{NH}_3/\text{H}_2$  blend was recommended due to low overall emissions and high stability at  $\Phi = 1.2$ .

## Declaration of competing interest

The authors declare that they have no known competing financial interests or personal relationships that could have appeared to influence the work reported in this paper.

## Acknowledgements

Cardiff University authors gratefully acknowledge the support from the EPSRC through the program Optimal fuel blends for ammonia fuelled thermal propulsion systems (EP/T033800/1). The experiments were undertaken at Cardiff University's Thermofluids Lab (W/0.07) with invaluable technical support from Mr. Malcolm Seaborne. Information on the data underpinning the results presented here, including how to access them, can be found in the Cardiff University data catalogue at <http://doi.org/10.17035/d.2022.0163135795>.

## REFERENCES

- [1] Valera-Medina A, Amer-Hatem F, Azad AK, Dedoussi IC, de Joannon M, Fernandes RX, et al. Review on ammonia as a potential fuel: from synthesis to economics. *Energy Fuels* 2021;35:6964–7029. <https://doi.org/10.1021/acs.energyfuels.0c03685>.
- [2] Hydrogen Council. Hydrogen insights [Online]. 2021. Available in: <https://hydrogencouncil.com/en/hydrogen-insights-2021/> [Accessed January 2021].
- [3] Cesaro Z, Ives M, Nayak-Luke R, Mason M, Bañares-Alcántara R. Ammonia to power: forecasting the leveled cost of electricity from green ammonia in large-scale power plants. *Appl Energy* 2021;282:116009. <https://doi.org/10.1016/j.apenergy.2020.116009>.
- [4] ETN. Hydrogen gas turbines. Brussels, Belgium. 2020 [Online]. Available in: <https://etn.global/wp-content/uploads/2020/01/ETN-Hydrogen-Gas-Turbines-report.pdf> [Accessed November 2021].
- [5] Kobayashi H, Hayakawa A, Somarathne KDKA, Okafor EC. Science and technology of ammonia combustion. *Proc Combust Inst* 2019;37:109–33. <https://doi.org/10.1016/j.proci.2018.09.029>.
- [6] Lhuillier C, Brequigny P, Lamoureux N, Contino F, Mounaïm-Rousselle C. Experimental investigation on laminar burning velocities of ammonia/hydrogen/air mixtures at elevated temperatures. *Fuel* 2020;263:116653. <https://doi.org/10.1016/j.fuel.2019.116653>.
- [7] Kanoshima R, Hayakawa A, Kudo T, Okafor EC, Colson S, Ichikawa A, et al. Effects of initial mixture temperature and pressure on laminar burning velocity and Markstein length of ammonia/air premixed laminar flames. *Fuel* 2022;310:122149. <https://doi.org/10.1016/j.fuel.2021.122149>.
- [8] Ji L, Wang J, Hu G, Mao R, Zhang W, Huang Z. Experimental study on structure and blow-off characteristics of  $\text{NH}_3/\text{CH}_4$

- co-firing flames in a swirl combustor. *Fuel* 2022;314:123027. <https://doi.org/10.1016/j.fuel.2021.123027>.
- [9] Haase H, Wald M. *Electrostatic hazards, their evaluation and control*. 2nd ed. New York: Verlag Chemie; 1977.
- [10] Pochet M, Foucher F, Jeanmart H, Contino F, Truedsson I. *Ammonia-hydrogen blends in homogeneous-charge compression-ignition engine*. 2017-24-0087. SAE International; 2017.
- [11] Zhang F, Chen G, Wu D, Zhang Z, Wang N. Characteristics of ammonia/hydrogen premixed combustion in a novel linear engine generator. *Proceedings* 2020;58. <https://doi.org/10.3390/WEF-06925>.
- [12] Sorrentino G, Sabia P, Bozza P, Ragucci R, de Joannon M. Low-NO<sub>x</sub> conversion of pure ammonia in a cyclonic burner under locally diluted and preheated conditions. *Appl Energy* 2019. <https://doi.org/10.1016/j.apenergy.2019.113676>.
- [13] Okafor EC, Yamashita H, Hayakawa A, Somarathne KDKA, Kudo T, Tsujimura T, et al. Flame stability and emissions characteristics of liquid ammonia spray co-fired with methane in a single stage swirl combustor. *Fuel* 2020;287:119433. <https://doi.org/10.1016/j.fuel.2020.119433>.
- [14] Mitsubishi Heavy Industries Group. Mitsubishi power commences development of world's first ammonia-fired 40MW class gas turbine system. 2021 [Online]. Available in: <https://power.mhi.com/news/20210301.html> [Accessed October 2021].
- [15] Rocha RC, Zhong S, Xu L, Bai X-S, Costa M, Cai X, et al. Structure and laminar flame speed of an ammonia/methane/air premixed flame under varying pressure and equivalence ratio. *Energy Fuels* 2021;35:7179–92. <https://doi.org/10.1021/acs.energyfuels.0c03520>.
- [16] Xiao H, Wang Z, Valera-Medina A, Bowen PJ. Study on characteristics of Co-firing ammonia/methane fuels under oxygen enriched combustion conditions. *J Therm Sci* 2018. <https://doi.org/10.1007/s11630-018-1008-1>.
- [17] Ramos CF, Rocha RC, Oliveira PM, Costa M, Bai XS. Experimental and numerical investigation on NO, CO and NH<sub>3</sub> emissions from NH<sub>3</sub>/CH<sub>4</sub>/air premixed flames. *Fuel* 2019;254:115693. <https://doi.org/10.1016/j.fuel.2019.115693>.
- [18] Mei B, Ma S, Zhang Y, Zhang X, Li W, Li Y. Exploration on laminar flame propagation of ammonia and syngas mixtures up to 10 atm. *Combust Flame* 2020;220:368–77. <https://doi.org/10.1016/j.combustflame.2020.07.011>.
- [19] Hewlett SG, Valera-Medina A, Pugh DG, Bowen PJ. Gas turbine co-firing of steelworks ammonia with coke oven gas or methane: a fundamental and cycle analysis. *Proc ASME Turbo Expo* 2019;3:GT2019–91404. <https://doi.org/10.1115/GT2019-91404>. Phoenix, Arizona.
- [20] Okafor EC, Somarathne KDKA, Ratthan R, Hayakawa A, Kudo T, Kurata O, et al. Control of NO<sub>x</sub> and other emissions in micro gas turbine combustors fuelled with mixtures of methane and ammonia. *Combust Flame* 2020;211:406–16. <https://doi.org/10.1016/j.combustflame.2019.10.012>.
- [21] Honzawa T, Kai R, Okada A, Valera-Medina A, Bowen PJ, Kurose R. Predictions of NO and CO emissions in ammonia/methane/air combustion by LES using a non-adiabatic flamelet generated manifold. *Energy* 2019;186:115771. <https://doi.org/10.1016/j.energy.2019.07.101>.
- [22] da Rocha RC, Costa M, Bai X-S. Chemical kinetic modelling of ammonia/hydrogen/air ignition, premixed flame propagation and NO emission. *Fuel* 2019;246:24–33. <https://doi.org/10.1016/j.fuel.2019.02.102>.
- [23] Ichikawa A, Hayakawa A, Kitagawa Y, Kunkuma Amila Somarathne KD, Kudo T, Kobayashi H. Laminar burning velocity and Markstein length of ammonia/hydrogen/air premixed flames at elevated pressures. *Int J Hydrogen Energy* 2015;40:9570–8. <https://doi.org/10.1016/j.ijhydene.2015.04.024>.
- [24] Lee JH, Kim JH, Park JH, Kwon OC. Studies on properties of laminar premixed hydrogen-added ammonia/air flames for hydrogen production. *Int J Hydrogen Energy* 2010;35:1054–64. <https://doi.org/10.1016/j.ijhydene.2009.11.071>.
- [25] Khateeb AA, Guiberti TF, Wang G, Boyette WR, Younes M, Jamal A, et al. Stability limits and NO emissions of premixed swirl ammonia-air flames enriched with hydrogen or methane at elevated pressures. *Int J Hydrogen Energy* 2021;46:11969–81. <https://doi.org/10.1016/j.ijhydene.2021.01.036>.
- [26] Valera-Medina A, Pugh DG, Marsh P, Bulat G, Bowen P. Preliminary study on lean premixed combustion of ammonia-hydrogen for swirling gas turbine combustors. *Int J Hydrogen Energy* 2017. <https://doi.org/10.1016/j.ijhydene.2017.08.028>.
- [27] Viguera-Zuniga M, Tejada-del-Cueto M, Vasquez-Santacruz J, Herrera-May A, Valera-Medina A. Numerical predictions of a swirl combustor using complex chemistry fueled with ammonia/hydrogen blends. *Energies* 2020;13:288. <https://doi.org/10.3390/en13020288>.
- [28] Goldmann A, Dinkelacker F. Experimental investigation and modeling of boundary layer flashback for non-swirling premixed hydrogen/ammonia/air flames. *Combust Flame* 2021;226:362–79. <https://doi.org/10.1016/j.combustflame.2020.12.021>.
- [29] Mashruk S, Xiao H, Valera-Medina A. Rich-Quench-Lean model comparison for the clean use of humidified ammonia/hydrogen combustion systems. *Int J Hydrogen Energy* 2020;46:4472–84. <https://doi.org/10.1016/j.ijhydene.2020.10.204>.
- [30] Keller M, Koshi M, Otomo J, Iwasaki H, Mitsumori T, Yamada K. Thermodynamic evaluation of an ammonia-fueled combined-cycle gas turbine process operated under fuel-rich conditions. *Energy* 2020;194:116894. <https://doi.org/10.1016/j.energy.2020.116894>.
- [31] Guteša Božo M, Mashruk S, Zitouni S, Valera-Medina A. Humidified ammonia/hydrogen RQL combustion in a trigeneration gas turbine cycle. *Energy Convers Manag* 2021;227:113625. <https://doi.org/10.1016/j.enconman.2020.113625>.
- [32] Joo JM, Kwon OCLS. Effects of ammonia substitution on combustion stability limits and NO<sub>x</sub> emissions of premixed hydrogen-air flames. *Int J Hydrogen Energy* 2012;37:6933–41. <https://doi.org/10.1016/j.ijhydene.2012.01.059>.
- [33] Um DH, Joo JM, Lee S, Kwon OC. Combustion stability limits and NO<sub>x</sub> emissions of nonpremixed ammonia-substituted hydrogen-air flames. *Int J Hydrogen Energy* 2013;38:14854–65. <https://doi.org/10.1016/j.ijhydene.2013.08.140>.
- [34] Tang G, Jin P, Bao Y, Chai WS, Zhou L. Experimental investigation of premixed combustion limits of hydrogen and methane additives in ammonia. *Int J Hydrogen Energy* 2021;46:20765–76. <https://doi.org/10.1016/j.ijhydene.2021.03.154>.
- [35] Celtek MS. The decreasing effect of ammonia enrichment on the combustion emission of hydrogen, methane, and propane fuels. *Int J Hydrogen Energy* 2022;47:9791–9. <https://doi.org/10.1016/j.ijhydene.2021.11.241>.
- [36] Li Z, Li S. Effects of inter-stage mixing on the NO<sub>x</sub> emission of staged ammonia combustion. *Int J Hydrogen Energy* 2022;47:9791–9. <https://doi.org/10.1016/j.ijhydene.2022.01.050>.
- [37] Khateeb AA, Guiberti TF, Zhu X, Younes M, Jamal A, Roberts WL. Stability limits and exhaust NO performances of ammonia-methane-air swirl flames. *Exp Therm Fluid Sci*

- 2020;114:110058. <https://doi.org/10.1016/j.exptthermflusci.2020.110058>.
- [38] Valera-Medina A, Marsh R, Runyon J, Pugh D, Beasley P, Hughes T, et al. Ammonia–methane combustion in tangential swirl burners for gas turbine power generation. *Appl Energy* 2017;185. <https://doi.org/10.1016/j.apenergy.2016.02.073>.
- [39] Pugh D, Valera-Medina A, Bowen P, Giles A, Goktepe B, Runyon J, et al. Emissions performance of staged premixed and diffusion combustor concepts for an nh<sub>3</sub>/air flame with and without reactant humidification. *J Eng Gas Turbines Power* 2020;1–10. <https://doi.org/10.1115/1.4049451>.
- [40] Netzer C, Ahmed A, Gruber A, Løvås T. Curvature effects on NO formation in wrinkled laminar ammonia/hydrogen/nitrogen-air premixed flames. *Combust Flame* 2021;232:111520. <https://doi.org/10.1016/j.combustflame.2021.111520>.
- [41] Dai L, Gersen S, Glarborg P, Mokhov A, Levinsky H. Autoignition studies of NH<sub>3</sub>/CH<sub>4</sub> mixtures at high pressure. *Combust Flame* 2020;218:19–26. <https://doi.org/10.1016/j.combustflame.2020.04.020>.
- [42] Zhang X, Wang J, Chen Y, Li C. Effect of CH<sub>4</sub> pressure, and initial temperature on the laminar flame speed of an NH<sub>3</sub>–air mixture. *ACS Omega* 2021;6:11857–68. <https://doi.org/10.1021/acsomega.1c00080>.
- [43] Zhu X, Khateeb AA, Guiberti TF, Roberts WL. NO and OH\* emission characteristics of very-lean to stoichiometric ammonia-hydrogen-air swirl flames. *Proc Combust Inst* 2021;38:5155–62. <https://doi.org/10.1016/j.proci.2020.06.275>. Elsevier Ltd.
- [44] Hayakawa A, Hayashi M, Gotama G, Kovaleva M, Okafor E, Colson Sophie, Mashruk Syed, Medina Valera, Agustin, Kobayashi H. N<sub>2</sub>O production characteristics of strain stabilized premixed laminar ammonia/hydrogen/air premixed flames in lean conditions. *13th Asia-Pacific Conf. Combust.*; 2021.
- [45] Mashruk S, Kovaleva M, Chong CT, Hayakawa A, Okafor E, Valera-Medina A. Nitrogen oxides as a by-product of ammonia/hydrogen combustion regimes. *Chem Eng Trans* 2021;89:613–8. <https://doi.org/10.3303/CET2189103>.
- [46] Glarborg P, Dam-Johansen K, Miller JA, Kee RJ, Coltrin ME. Modeling the thermal DENOx process in flow reactors. Surface effects and Nitrous Oxide formation. *Int J Chem Kinet* 1994;26:421–36. <https://doi.org/10.1002/kin.550260405>.
- [47] He X, Shu B, Nascimento D, Moshhammer K, Costa M, Fernandes RX. Auto-ignition kinetics of ammonia and ammonia/hydrogen mixtures at intermediate temperatures and high pressures. *Combust Flame* 2019. <https://doi.org/10.1016/j.combustflame.2019.04.050>.
- [48] Alturaifi SA, Mathieu O, Petersen EL. Shock-tube laser absorption measurements of N<sub>2</sub>O time histories during ammonia oxidation. *Fuel Commun* 2022:100050. <https://doi.org/10.1016/j.fueco.2022.100050>.
- [49] Shu B, He X, Ramos CF, Fernandes RX, Costa M. Experimental and modeling study on the auto-ignition properties of ammonia/methane mixtures at elevated pressures. *Proc Combust Inst* 2020. <https://doi.org/10.1016/j.proci.2020.06.291>.
- [50] Stagni Alessandro, Cavallotti Carlo, Arunthanayothin Suphaporn, Song Yu, Herbinet Olivier, Battin-Leclerc Frédérique, et al. An experimental, theoretical and kinetic-modeling study of the gas-phase oxidation of ammonia. *React Chem Eng* 2020;5:696–711. <https://doi.org/10.1039/C9RE00429G>.
- [51] Valera-Medina A, Banares-Alcantara R. *Techno-economic challenges of ammonia as energy vector*. 1st ed. Academic Press; 2020.
- [52] ETN. FLEXnCONFU. 2020 [Online]. Available in: <https://flexnconfu.eu> [Accessed May 2021].
- [53] Okafor EC, Somarathne KDKA, Hayakawa A, Kudo T, Kurata O, Iki N, et al. Towards the development of an efficient low-NOx ammonia combustor for a micro gas turbine. *Proc Combust Inst* 2019;37:4597–606. <https://doi.org/10.1016/j.proci.2018.07.083>.
- [54] Costa M, Ramos F, Rocha R, Oliveira P, Bai X-S. *Ammonia combustion: experiments and kinetic studies*. Dubrovnik, Croatia: 14th Int. SDEWES Conf.; 2019.
- [55] Khateeb AA, Guiberti TF, Zhu X, Younes M, Jamal A, Roberts WL. Stability limits and NO emissions of technically-premixed ammonia-hydrogen-nitrogen-air swirl flames. *Int J Hydrogen Energy* 2020;45:22008–18. <https://doi.org/10.1016/j.ijhydene.2020.05.236>.
- [56] Valera-Medina A, Morris S, Runyon J, Pugh DG, Marsh R, Beasley P, et al. Ammonia, methane and hydrogen for gas turbines. *Energy Proc* 2015;75. <https://doi.org/10.1016/j.egypro.2015.07.205>.
- [57] Gaydon A. *The spectroscopy of flames*. Springer; 2012. p. 424.
- [58] Ohashi K, Kasai T, Che DC, Kuwata K. Alignment dependence of the amidogen chemiluminescence in the reaction of argon(3P) atoms with the aligned ammonia molecules. *J Phys Chem* 2002;93:5484–7. <https://doi.org/10.1021/J100351A033>.
- [59] Schott GL, Blair LS, JDM Jr. Exploratory shock-wave study of thermal nitrogen trifluoride decomposition and reactions of nitrogen trifluoride and dinitrogen tetrafluoride with hydrogen. *J Phys Chem* 2002;77:2823–30. <https://doi.org/10.1021/J100642A001>.
- [60] Roose TR, Hanson RK, Kruger CH. A shock tube study of the decomposition of no in the presence of NH<sub>3</sub>. *Symp Combust* 1981;18:853–62. [https://doi.org/10.1016/S0082-0784\(81\)80089-6](https://doi.org/10.1016/S0082-0784(81)80089-6).
- [61] Yi Y, Zhang R, Wang L, Yan J, Zhang J, Guo H. Plasma-triggered CH<sub>4</sub>/NH<sub>3</sub> coupling reaction for direct synthesis of liquid nitrogen-containing organic chemicals. *ACS Omega* 2017. <https://doi.org/10.1021/acsomega.7b01060>.
- [62] Mashruk S. NO formation analysis using chemical reactor modelling and LIF measurements on industrial swirl flames - PhD thesis. Cardiff University; 2020. <https://doi.org/10.13140/RG.2.2.28297.06246/1>.
- [63] Maas U, Warnatz J. Ignition processes in hydrogen oxygen mixtures. *Combust Flame* 1988;74:53–69. [https://doi.org/10.1016/0010-2180\(88\)90086-7](https://doi.org/10.1016/0010-2180(88)90086-7).
- [64] Stahl G, Warnatz J. Numerical investigation of time-dependent properties and extinction of strained methane and propane-air flamelets. *Combust Flame* 1991;85:285–99. [https://doi.org/10.1016/0010-2180\(91\)90134-W](https://doi.org/10.1016/0010-2180(91)90134-W).
- [65] Eckart S, Yu C, Maas U, Krause H. Experimental and numerical investigations on extinction strain rates in non-premixed counterflow methane and propane flames in an oxygen reduced environment. *Fuel* 2021;298:120781. <https://doi.org/10.1016/j.fuel.2021.120781>.
- [66] Li R, Konnov AA, He G, Qin F, Zhang D. Chemical mechanism development and reduction for combustion of NH<sub>3</sub>/H<sub>2</sub>/CH<sub>4</sub> mixtures. *Fuel* 2019. <https://doi.org/10.1016/j.fuel.2019.116059>.
- [67] Valera-Medina A, Gutesa M, Xiao H, Pugh D, Giles A, Goktepe B, et al. Premixed ammonia/hydrogen swirl combustion under rich fuel conditions for gas turbines operation. *Int J Hydrogen Energy* 2019;44:8615–26. <https://doi.org/10.1016/j.ijhydene.2019.02.041>.
- [68] Ichimura R, Hadi K, Hashimoto N, Hayakawa A, Kobayashi H, Fujita O. Extinction limits of an ammonia/air flame propagating in a turbulent field. *Fuel* 2019;246:178–86. <https://doi.org/10.1016/j.fuel.2019.02.110>.

- [69] Jiang H, Bi M, Gao Z, Zhang Z, Gao W. Effect of turbulence intensity on flame propagation and extinction limits of methane/coal dust explosions. *Energy* 2022;239:122246. <https://doi.org/10.1016/j.energy.2021.122246>.
- [70] Zitouni S-E, Mashruk S, Mukundakumar N, Brequigny P, Zayoud A, Pucci E, et al. Ammonia blended fuels - energy solutions for a green future. In: *Gas turbines a carbon-neutral Soc. 10th Int. Gas Turbine Conf.*; 2021. IGTC21–62.
- [71] Konnov AA. Yet another kinetic mechanism for hydrogen combustion. *Combust Flame* 2019. <https://doi.org/10.1016/j.combustflame.2019.01.032>.
- [72] Bonciolini G, Faure-Beaulieu A, Bourquard C, Noiray N. Low order modelling of thermoacoustic instabilities and intermittency: flame response delay and nonlinearity. *Combust Flame* 2021;226:396–411. <https://doi.org/10.1016/j.combustflame.2020.12.034>.
- [73] Becker K, Lörzer J, Kurtenbach R, Wiesen P, Jensen T, Wallington T. Contribution of vehicle exhaust to the global N<sub>2</sub>O budget. *Chemosphere Global Change Sci* 2000;2:387–95. [https://doi.org/10.1016/S1465-9972\(00\)00017-9](https://doi.org/10.1016/S1465-9972(00)00017-9).
- [74] Glarborg P, Miller JA, Ruscic B, Klippenstein SJ. Modeling nitrogen chemistry in combustion. *Prog Energy Combust Sci* 2018;67:31–68. <https://doi.org/10.1016/j.pecs.2018.01.002>.
- [75] Valera-Medina A, Gutesa M, Xiao H, Pugh D, Giles A, Goktepe B, et al. Premixed ammonia/hydrogen swirl combustion under fuel-rich conditions for gas turbines operation. *Proc Combust Inst* 2018:8615–26. <https://doi.org/10.1016/j.ijhydene.2019.02.041>. under revi.
- [76] Somarathne KDKA, C. Okafor E, Hayakawa A, Kudo T, Kurata O, Iki N, et al. Emission characteristics of turbulent non-premixed ammonia/air and methane/air swirl flames through a rich-lean combustor under various wall thermal boundary conditions at high pressure. *Combust Flame* 2019;210:247–61. <https://doi.org/10.1016/j.combustflame.2019.08.037>.
- [77] Mashruk S, Xiao H, Pugh D, Chiong M-C, Runyon J, Goktepe B, et al. Numerical analysis on the evolution of NH<sub>2</sub> in ammonia/hydrogen swirling flames and detailed sensitivity analysis under elevated conditions. *Combust Sci Technol* 2021. <https://doi.org/10.1080/00102202.2021.1990897>.